

We are IntechOpen, the world's leading publisher of Open Access books Built by scientists, for scientists

6,900

Open access books available

186,000

International authors and editors

200M

Downloads

Our authors are among the

154

Countries delivered to

TOP 1%

most cited scientists

12.2%

Contributors from top 500 universities



WEB OF SCIENCE™

Selection of our books indexed in the Book Citation Index
in Web of Science™ Core Collection (BKCI)

Interested in publishing with us?
Contact book.department@intechopen.com

Numbers displayed above are based on latest data collected.
For more information visit www.intechopen.com



CFD as a Tool for the Analysis of the Mechanical Integrity of Light Water Nuclear Reactors

Hernan Tinoco

Additional information is available at the end of the chapter

<http://dx.doi.org/10.5772/52691>

1. Introduction

The analysis of the mechanical integrity of Light Water Nuclear Reactors has experienced a strong evolution in the two latest decades. Until the nineteen eighties, the structural design was practically based on static loads with amplifying factors to take dynamic effects into account, (see e. g. Lahey and Moody, 1993), and on wide safety margins. Even if an incipient methodology for studying earthquake effects already existed, it was only at the end of the nineties when a complete analysis about dynamic loads, caused by a steam line guillotine-break of a BWR, was carried out for the first time (Hermansson and Thorsson, 1997). This analysis, based on a three-dimensional Computational Fluid Dynamic (CFD) simulation of the break, revealed a discrepancy with former applied loads that had never been exposed in the past due to inappropriate experimental setup geometry (Tinoco, 2001). In addition, the analysis pointed out the importance of also studying the load frequencies. The complete issue is further discussed in Section 3.

Nonetheless, CFD has shown to be a much more versatile tool. Issues like checking the maximum temperature of the core shroud of the reactor, when the power of the reactor is uprated (Tinoco et al., 2008), or estimating the thermal loadings during different transient conditions when the Emergency Core Cooling System (ECCS) has been modified, (Tinoco et al., 2005), or studying the automatic boron injection during an Anticipated Transient Without Scram (ATWS), (Tinoco et al., 2010a), have all been settled by means of CFD simulations.

Even more significantly, a rather complete CFD model of the Downcomer, internal Main Recirculation Pumps (MRP) and Lower Plenum up to the Core Inlet, (Tinoco and Ahlinder, 2009), has shed some light concerning the thermal mixing in the different regions of the reactor and also about the appropriateness of using connected sub-models as constituting parts of a larger model. The complete matter of thermal mixing is discussed in detail in Section 4.

Last but not least, CFD has demonstrated that it can be used to establish the causes of component failure. Even if justified suspicions existed about the cause of two broken control rods and of a large number of rods with cracks at the twin reactors Oskarshamn 3 and Forsmark 3, no knowledge existed about the details of the failure process (Tinoco and Lindqvist, 2009). It was first when time dependent CFD simulations revealed the structure of the thermal mixing process in the control rod guide tube that the cause, thermal fatigue of the rods, was confirmed and understood (Tinoco and Lindqvist, 2009, Tinoco et al., 2010b, Angele et al., 2011). This subject, together with the general problem of conjugate heat transfer, is analysed in Section 5.

Firstly, this chapter intends to communicate an historical view of CFD applied to the analysis of the mechanical integrity of Light Water Nuclear Reactors. Secondly, the chapter examines and evaluates several methodologies and approaches corresponding to the present and future modelling in the field of thermal hydraulics related to this type of analysis.

2. The determination of loadings

Considering the devastating effect that uncontrolled loadings may have on life and property, this section will begin by evoking the history of pressure vessel advance. This road to progress is paved with disastrous accidents which, during the decade of the eighteen eighties, amounted in the USA to more than 2000 boiler explosions. The establishment of ASME in February 1880 was, according to legend, directly prompted by the need to solve the problem of unsafe boilers (Varrasi, 2005). But it was first after the explosion on March 20, 1905, of the boiler of the R. B. Grover & Company Shoe Factory in Brockton, Massachusetts, (see Fig. 1 below, USGenWeb, 2011, Ellenberger et al., 2004) that the real effort of developing rules and regulations for the construction of secure steam boilers speeded up, urged by the public opinion. During the subsequent years, many states legislated, without too much coordination, about what was considered suitable instructions and procedures, leading to inconsistency in the construction requirements. Finally, in the spring of 1915, the first *ASME Rules for Construction of Stationary Boilers and For Allowable Working Pressures* consisting of one book of 114 pages, known as the 1914 edition, was made available, and the path towards regulation uniformity commenced.



Figure 1. View of the R. B. Grover & Company Shoe Factory before (left) and after (middle and right) the boiler explosion on March 20, 1905, that killed 58 persons and injured 117, (USGenWeb, 2011, Ellenberger et al., 2004).

Since then, the ASME Code has become both larger and more comprehensive, comprising today 28 books, with 12 books dedicated to the Construction and Inspection of Nuclear Power Plant Components. Fortunately, even the boiler explosion trend in the USA has radically changed since 1905, as Figure 2 below shows.

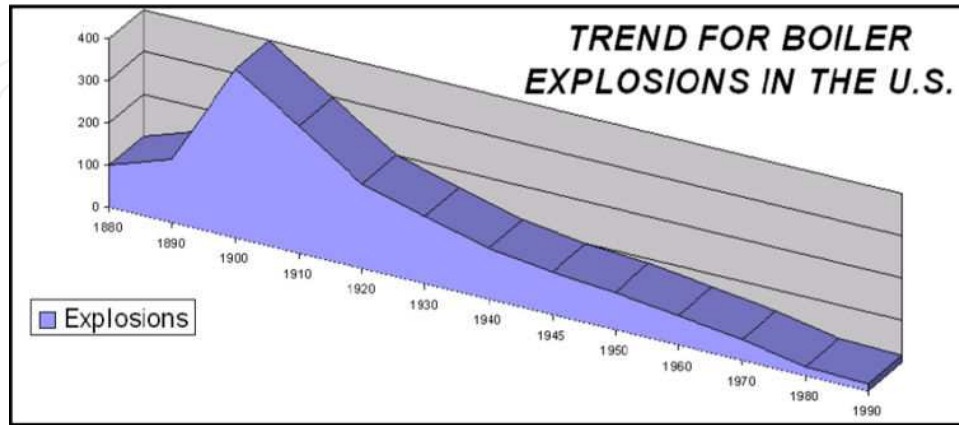


Figure 2. Trend for boiler explosions in the USA (from Hill, 2008).

For nuclear applications, the complete ASME code is mandatory only in the USA. In the European Union, on the other hand, no coordination process has been agreed. The Pressure Equipment Directive, (EU, 1997), has been adopted by the European Parliament and the European Council for harmonizing the national laws of Member States to promote and facilitate trade and exchange between States. But in the nuclear field, the application limits of the Directive and the Nuclear Codes (possibly ASME) have to be agreed with the National Nuclear Regulatory Authorities.

2.1. Section III

The ASME Boiler and Pressure Vessel Code, Section III, Rules for Construction of Nuclear Power Plant Components, of which the last Edition is from 2010, (ASME, 2010), regulates the design and construction of nuclear facility components. This Section “provides requirements for the materials, design, fabrication, examination, testing, inspection, installation, certification, stamping, and overpressure protection of nuclear power plant components, and component and piping supports. Components include metal vessels and systems, pumps, valves, and core support structures.”

Section III comprises Divisions 1, 2 and 3 and the introductory Subsection NCA that specifies General Requirements for Divisions 1 and 2. Division 1 contains eight Subsections, namely NB, for Class 1 Components, NC, for class 2 Components, ND, for class 3 Components, NE, for class MC Components, NF, for Supports, NG, for Core Support Structures, NH, for Class 1 Components in Elevated Temperature Service, and Appendices, both mandatory and nonmandatory, including, inter alia, a listing of design and design analysis methods.

2.2. Categorisation of parts in code classes

The aforementioned Code classes are proposed for the categorisation of parts of a nuclear power system, in accordance with the level of importance related to their function in the safe operation of the plant. However, the Code does not provide guidance for classifying the different parts. Classification, which is the responsibility of the Owner, has to be achieved by applying system safety criteria to be found in engineering standards and/or requirements of the Nuclear Regulatory Authorities. For instance, Class 1 components are those that are part of the primary core cooling system, or components that are used in elevated temperature service, and are constructed in accordance with the rules of Subsection NB. Class 2 components are those that are part of various important-to-safety emergency core cooling systems, and are constructed in accordance with the rules of Subsection NC. Class 3 components are those that are part of the various systems needed for plant operation, and are constructed in accordance with the rules of Subsection ND. Class MC components are metal containment vessels constructed in conformity with the rules of Subsection NE. Class CS components are core support structures constructed in accordance with the rules of Subsection NG. Mandatory and/or nonmandatory modifications and/or extensions to these classes may be included by Nuclear Regulatory or other Authorities, (STUK, 2000, IAEA, 2010).

2.3. Mechanical integrity and design specifications

The requirements for mechanical integrity are based on Norms and aim at ensuring that nuclear components shall withstand pressure and other types of loadings without system break or leakage. The Class to which the component belongs to shall govern the choice of Norms that are used for the analysis of its mechanical integrity. Design Specifications for mechanical integrity shall indicate the Loadings and Loading Combinations that a mechanical component is submitted to and, at the same time, the acceptable level of the Loadings and Loading Combinations, i.e. Loading Limits.

Within the realm of the ASME Code, the introductory Subsection NCA covers “general requirements for manufacturers, fabricators, installers, designers, material manufacturers, material suppliers, and owners of nuclear power plants”, (ASME, 2010). Here, Subsection NCA-2142 imposes to the Owner or his designee the duty of “identify the Loadings and combinations of Loadings and establish the appropriate Design, Service, and Test Limits for each component or support”. For this purpose, Loadings are separated into Design, Service and Test Loadings, and their Limits correspond to the acceptable Loadings permitted in a structural analysis. General directions about the characterization of Design, Service and Test Limits may be found in Subsection NCA-2142.4.

In order to be able to determine the Loadings that a component or support is submitted to, the different operating conditions that may affect the component or support have to be defined. The selection should include Normal Operation, Abnormal Conditions and Accidents that the component or support shall successfully withstand. Also, to be able to estimate the Limits that the Loadings must conform to, each operation condition must be related to an occurrence probability, being a lower probability associated with higher acceptable Limits. This matter may be solved by an event classification such as that of ANSI/ANS (1983a) for

PWR and ANSI/ANS (1983b) for BWR. Here, Plant Condition PC1 corresponds to normal operating conditions, PC2 to anticipated conditions (occurrence frequency of $> 10^{-2}$ times/year), PC3 to abnormal operating conditions (occurrence frequency of $10^{-2} - 10^{-4}$ times/year), PC4 to postulated accidents (occurrence frequency of $10^{-4} - 10^{-6}$ times/year) and PC5 to low probability accidents (occurrence frequency of $10^{-6} - 10^{-7}$ times/year).

2.4. Design loadings and limits

Subsection NCA-2142.1 indicates that the Design Loadings shall be specified by stipulating (a) the Design Pressure, (b) the Design Temperature and (c) the Design Mechanical Loads. External and internal Design Pressure shall be consistent with the maximum pressure difference between the inside and outside of the item, or between any two chambers of a combination unit. The Design Temperature shall be equal to or higher than the expected maximum thickness-mean metal temperature of the part considered. The Design Mechanical Loads “shall be selected so that when combined with the effects of Design Pressure, they produce the highest primary stresses of any coincident combination of loadings for which Level A Service Limits (see below about limits) are designated in the Design Specification”. Primary stresses are those arising from the imposed loading, not those developed by constraining the free displacement of the structural system. Primary stresses are necessary to satisfy the mechanical equilibrium of the system. The component or support shall be structurally analysed for the Loadings associated with Design Pressure, Design Temperature and Design Mechanical Loads where, in general, their possible cyclic or transient behaviour is not included.

Design Limits shall designate the limits for Design Loadings. The Limits for Design Loadings shall conform to the requisites given in the applicable Subsection of Section III, i.e. NB, NC, ND, NE, NF or NG. In the event of Loadings that are not structurally analysed, the Limits are set to the same level as Service Limits A (see below).

2.5. Service loadings and limits

From the defined operation conditions, the Service Loadings may now be derived. Service Loadings are all loadings that a component is subject to under predictable normal and abnormal operational conditions and postulated accidents that have to be included in the Design Specification. More specifically, Service Loadings are pressure, temperature loads, mechanical loads and their possible cyclic or transient behaviour (see e.g. Subsection NCA-2142.2). Related loadings shall be integrated in Service Loading Combinations which, together with the corresponding Plant Condition or assigned probability, shall be assessed against relevant Limits.

According to Subsection NCA-2142-3, Service Limits are divided into four levels, namely Service Limits A, B, C and D. Service Limit A corresponds to bounds that contain the safety margins and factors that are required for the component to completely fulfil the specified performance. Service Limit B corresponds to bounds that contain smaller safety margins and factors than Limit A, but that still ensure a component free from damage. Service Limits C

and D correspond to bounds with even more reduced safety margins and factors that now may lead to permanent deformation and damage of the component, a situation requiring repair of the component. The last two Limit levels may not be suitable for pressure vessels since their mechanical integrity should not be jeopardised.

The Plant Conditions (operation conditions together with their corresponding occurrence probability) shall decide which Limit to be applied. This coupling shall be account for in the Safety Analysis of the system (see e.g. ANSI/ANS 51.1 or ANSI/ANS 52.1, Appendix 2).

In the evaluation of a component according to Section III, Subsections NB, NC, ND, NE, NF or NG, quantifying values corresponding to Service Limits A to D shall be assigned to the allowed stresses.

2.6. Test loadings and limits

Test Loadings correspond to all Loadings that a component is subjected to during the tests that the component has to undergo. In general, these correspond to pressure tests but, if other types of tests are required, these must be stated in the Design Specification (see Subsection NCA-2142.3).

Test Limits indicate bounds for the tests to be performed on a component. In the evaluation of a component according to Section III, Subsections NB, NC, ND, NE, NF or NG, quantifying values corresponding to the Test Limits shall be assigned to the allowed stresses.

2.7. Load combinations

The overall-categorized Loadings with their corresponding Limits comprise a part of the background necessary to accomplish a structural analysis. Its complementary part is constituted by Load Combinations, the definition of which is, according to NCA-2142, a responsibility of the Owner of the Nuclear Facility, or of his designee. The combination of already identified Loads has to consider the type of Load, i.e. static or dynamic, global or local. In addition, the combination has to determine if they are consecutive or simultaneous, i.e. pressure and temperature loads related to a Loss of Coolant Accident (LOCA). Also, the time history of each Load shall be taken into account in order to prevent an unlikely superposition of non-simultaneous peaks. Eventually, the occurrence probability of each load combination shall be assessed.

Consequently, Design Conditions may include not only static loads like Design Pressure (DP), Design Temperature (TD) and Dead Weight (DW) but also dynamic loads like those generated by, for instance, the opening/closing of one safety valve (GV/SRV(1)). In the combination notation, the number of valves involved is indicated within parenthesis. Also, the occurrence probability of the maximum load may be added as the inverse of the number of valve activations under which this maximum is achieved, for instance “ $\geq E-3$ ”, meaning the maximum load in 1000 activations (see e.g. Table 1).

More specifically, the loadings due to Operational Transients and Postulated Accidents may, for instance, include the Operation Pressure (PO), the Operation Temperature (TO),

temperature transient (TT), joint displacement of reactor nozzle (D/RPV), building displacement (DB), condensation-induced water hammer when starting the high pressure Emergency Core Cooling (HP-ECCS) system or the Feed Water System (WH/SC), water hammer by star/stop of a pump (WH/PT) and global vibration due to safety valve discharge (GV/SRV).

The loadings due to Postulated Accidents may also include water hammer caused by a pipe break external to the Containment (WH/PBO), reactor vibrations generated by internal pipe break in the Containment (PRVV/PBI), global vibrations due to condensation oscillations in the suppression pool (GV/CO) and global vibration by condensation-induced pressure pulses, chugging, in the suppression pool, (GV/CH). Finally, loads caused by other incidents may be those corresponding to global vibrations due to Safe-Shutdown Earthquake (GV/SSE).

In a linear structural analysis, the effect of a Load Combinations is evaluated by a simple linear superposition of the response of each normal mode, separately analysed, through the procedure referred to as modal analysis. In cases where the time dependent functions of Loads acting simultaneously are statistically independent of each other, an upper bound of the total response may be estimated by a method denoted Square Root of Sum of Squares (SRSS), and not by the very conservative linear sum of the maxima. If the structural analysis is non-linear, as in Zeng et al. (2011), modal analysis is no longer valid and Collapse-Load analysis, together with non-linear Transient analysis, is required.

Combination	Superposition Rule	Plant Condition	Service Limit Levels
A01	PD + DW	–	Design
A03	PO + DW + TT + D/RPV + D/B	PC1/PC2	A/B
A06	PO + DW + GV/SRV(1)	PC1	Design, A
A07a	PO + DW + GV/SRV(12 ≥ E-3)	PC2	B
A07b	PO + DW + GV/SRV(12 ≥ E-8)	PC4	D
A08a	PO + DW + GV/SRV(12 ≥ E-2)	PC3	C
A09a	PO + DW + WH/SC	PC2	B
A09b	PO + DW + WH/SC	PC3	C
A11	PO + DW + WH/PBO	PC4	D
A13	$PO + DW + [(GV/SRV(1))^2 + (GV/CO)^2]^{1/2}$	PC4	D
A14	$PO + DW + [(GV/SRV(1))^2 + (GV/CH)^2]^{1/2}$	PC4	D
A16	$PO + DW + [(GV/SRV(12 \geq E-3))^2 + (RPVV/PBI)^2]^{1/2}$	PC4	D
A17	$PO + DW + [(GV/SRV(12 \geq E-2))^2 + (GV/SSE)^2]^{1/2}$	PC5	D

Table 1. Design Specifications for the feed water system (System 415) of a BWR (Forsmark 1, Forsmarks Kraftgrupp, 2007).

As an example of Design Specifications for pressure- and force-bearing components, Table 1 shows the different Load Combinations corresponding to a part of the feed water system of an internal pump BWR corresponding to Unit 1 of Forsmark Nuclear Power Plant (NPP). In this table, some of the Load combinations appear to be identical but they actually differ in, for instance, the pressure and/or temperature limits. For the sake of simplicity, this information has not been included in the table. It might be of some interest to point out that the Case A17 corresponds to a combination of an earthquake from San Francisco, USA, and another from Sweden, since the spectra of these earthquakes differ in the frequency content. This Combination has a Plant Condition PC5 for the Swedish reality, for which a safe shutdown of the reactor must be guaranteed.

Forsmark is the youngest Swedish NPP that became operational in 1980 with Unit 1 and whose installed power was completed in 1985 with the start of Unit 3. This Unit and Unit 3 of Oskarshamn NPP were the last reactors to be built in Sweden. These two internal pump reactors were designed at the end of the nineteen sixties and beginning of seventies, when the first pocket calculators begun to invade the market. But these calculators were initially quite expensive (Hewlett-Packard's HP-35 cost \$395 in 1972 which corresponds today to more than \$2000), forcing the structural analyses to the use of rather simplified rough models, such as columns and beams subjected mainly to static loads, computed by means of slide rules. Dynamical effects were considered using a quasi-static approach with adequate safety margins (see e.g. Lahey and Moody, 1993), constituting the only feasible and realistic conservative approach compatible with the existing algorithms and computer capacity of the time. Nevertheless, thanks to the increased knowledge in the physics of single- and multi-phase flows, to the development of numerical models for fluids and structures together with the massive computing power through parallelization and low-price processers, mechanical integrity analysis of Light Water Nuclear Reactors has, during the two last decades, experienced a strong progress.

As discussed above, a nuclear reactor is designed for normal steady-state operation, for normal changes such as start-up, shutdown, change in power level, etc., without going beyond the design limits. In addition, the design must manage expected abnormal conditions and postulated accidents. In this context and according to Lahey and Moody (1993), an accident "is defined as a single event, not reasonably expected during the course of plant operation, that has been hypothesized for analysis purposes or postulated from unlikely but possible situations and that has the potential to cause a release of an unacceptable amount of radioactive material". Consequently, a break in the reactor coolant system has to be considered an accident whereas a fuel cladding tube damage is not.

Among postulated accidents, a group known as Anticipated Transients Without Scram (ATWS), has a preferential status due to the interest that it has attracted since the end of the nineteen seventies. It assumes the partial or total failure of the automatic control rod insertion (SCRAM). A total ATWS has a very low occurrence probability in the reactors of Forsmark NPP. The total of about 170 control rods is divided into independent scram groups, each served by a scram module and containing eight to ten control rods. A scram module consists of a high-pressure nitrogen tank connected by a scram valve to another tank con-

taining water to be pressurized by the nitrogen, water that may act on piston tubes for accomplishing rapid insertion of control rods. It might be of some interest to point out that similar scram systems successfully stopped units 2, 3, 4 and 7 of the Kashiwazaki-Kariwa NPP in Japan at the beginning of the earthquake Chūetsu of July 16, 2007 (the remaining units 1, 5 and 6 and were not operational due to refuelling outage). Still, Forsmark's Units have an independent system of boron injection for emergency stop of the reactors, which is automated for Units 1 and 2 but still manual for Unit 3. Although the automation of this system, which was a Regulatory compliance, is not associated with safety issues, can, nevertheless, lead to new thermal loads for the fuel and/or adjacent structures in the reactor core (Tinoco et al., 2010a). As mentioned above, it is the duty of the owner or designee of the nuclear facility to identify the Mechanical Loadings and/or their Combinations and establish appropriate Limits. It is therefore necessary to analyse the effects of boron injection, a topic to be discussed in somewhat more detail in Section 3 of this chapter.

The design basis accident of an external pump Boiling Water Reactor (BWR) consists of a two-ended instantaneous circumferential break on the suction side of one of the main recirculation lines, resulting in a discharge from both ends. In a BWR with internal pumps, this postulated accident is not possible since there are no main recirculation lines. For an internal pump BWR, there no longer exists a single design basis accident, but rather a series of accidents, whose consequences for safety and mechanical integrity are at least an order of magnitude smaller than the rupture of a main recirculation line. One of these accidents consists of the two-ended instantaneous circumferential break of a steam line, which produces the highest loads in the vessel and reactor internals. A similar break of a feedwater line will result in lower Loads due to damping two-phase effects, in this case mainly from rapid boiling, i.e. flashing. Therefore, a design basis accident to be analysed for an internal pump BWR is a steam line break that will be discussed in more detail in the following Section.

3. A steam line break

Until the mid-nineties, studies and analysis of the effects of a steam line break were mainly based on experiments such as those of The Marviken Full Scale Critical Flow Tests (1979) where the pressure vessel consisted of a cylindrical tank with no internal parts, filled only with steam. For this reason, the only pressure waves considered in the loading analyses were the alternating decompression and compression waves formed in the pipe segment coupled to the cylindrical tank, between the break section and the coupling section to the tank (see for example Lahey and Moody, 1993, pp. 498-501). Consequently, the Loads given by the standard ANSI/ANS-58.2-1988, (ANSI/ANS, 1988), contain a component due to pressure waves of slightly over 30% of the product of the initial pressure of the cylindrical tank times the area of the section break. That the presence of the concentric steam annulus between the reactor vessel and the core shroud has an important part in the process of decompression by supporting standing pressure waves, (Tinoco, 2001), has been understood after the CDF analysis to be briefly describe in what follows.

A three-dimensional numerical analysis of the rapid transient corresponding to the rupture of the steam line (Tinoco, 2002) started in the late nineties with the purpose of obtaining the time signal of the pressure inside the reactor pressure vessel and its internals, to be later used in a structural time history analysis. This work was motivated as a part of the structural analysis related to replacement of the core grid of Units 1 and 2 of Forsmark NPP from the original, fabricated by welded parts that had developed cracks in the welds, to a new manufactured in one piece.

Historically, the three-dimensional numerical simulation of the fast transient was one of the first successes in this area of thermal-hydraulics. This was due to several factors that allowed an analysis with relatively limited computational resources, namely a negligible effect of turbulence, single-phase treatment due to flashing delay and the lack of importance of friction allowing relatively coarse mesh (see Tinoco, 2002).

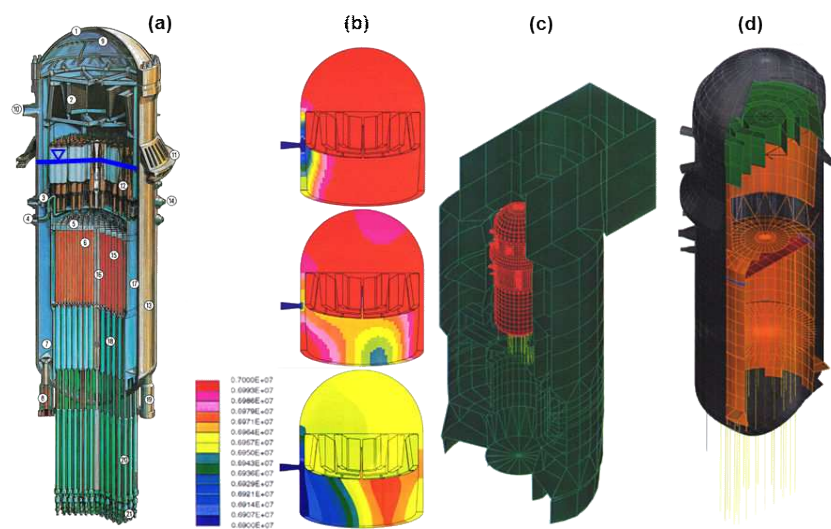


Figure 3. (a) View of the reactor with water surface indicated by blue line, (b) Model of the steam dome, annulus and dryers (down to water surface) after steam line break: 9 ms (upper view), 20 ms (central view) and 100 ms (lower view), (c) Simplified FEM model of the reactor with containment building, (d) detailed FEM model of the reactor with core grid in red.

Figure 3 shows in (a) an image of the reactor with the water surface indicated by a blue line. In (b) this figure shows a sequence of views of the pressure on the inner surface of the numerical model CFD ("Computational Fluid Dynamics") model (Tinoco, 2002), containing the steam dome, the annular region of steam and steam dryers. The steam separators, located under the dryers were modelled together as a single barrel without details. The first view of the sequence corresponds to 9.2 ms after the break, where the decompression wave extends with a single front symmetrically with respect to the axis of the steam nozzle, on whose outer end the line break is assumed to be located. The second view corresponds to 20.2 ms after the break, showing a picture of a less ordered and more chaotic pressure field due to reflections with different parts of the complex geometry of the reactor vessel. The third view corresponds to 100 ms from the break, displaying a more simplified image of the pressure than

in the previous view, due mainly to the general decompression of the reactor that has almost homogenised the dome pressure. Image (c) shows a general view of the low-resolution structural analysis FEM model, including the containment building. Image (d) shows a view of the high-resolution FEM model of the reactor.

A structural analysis was performed using both models because, due to the rupture of the steam line, there is an effect, external to the reactor vessel, on the reactor containment building, not considered in Tinoco (2002) since it only treats internal effects. The analysis was conducted using the method of direct time integration, (Hermansson and Thorsson, 1997). The time signals of the loads were applied to the structures and, as a result, response spectra were generated for the different structures. A response spectrum is a graph of the maximal response (displacement, velocity or acceleration) of a linear oscillatory system (elastic structure) forced to move by a vibrational excitation or pulse (shock). Figure 4 shows in (a) two time signals of load components in the direction of the axis of the steam nozzle with the line break, acting on a node located in the core grid. The lower value corresponds to that computed directly by the CFD model. The higher, amplified value takes into account the effect of the second end of the break, which is connected to the adjacent steam line (Hermansson and Thorsson, 1997). Due to this connection in pairs of the steam lines, the reactor vessel is also decompressed, with a certain delay, through the contiguous steam nozzle. In (b), Figure 4 shows the smoothed envelope spectra in the direction of the axis of the steam nozzle with the line break, corresponding to the same node. It might be of some interest to reiterate that the loads applied in this analysis are about twice the loads according to standard ANSI/ANS-58.2-1988, (ANSI/ANS,1988), due to an effect of resonance of pressure waves in the steam annulus (Tinoco, 2001).

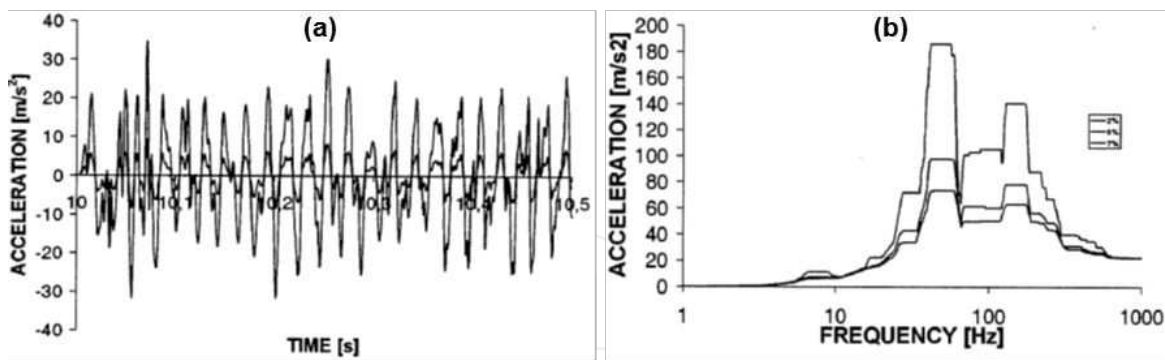


Figure 4. (a) Time signals of the acceleration of a node in the core grid in the direction of the axis of the steam nozzle with break: value calculated by CFD and amplified value. (b) Smoothed envelope spectra in in the direction of the axis of the steam nozzle with break for the same node in the core grid.

4. The problem of mixing

Mixing the same fluid with different properties like temperature or concentration, or with different phases like steam and water, or even different fluids, is a far from trivial industrial

problem. The process involved in the operation of Light Water Reactors contains many situations where mixing is of crucial importance like the mixing of reactor water and feedwater in BRWs, the mixing needed to regulate boron concentration in PWRs, etc. Yet, a high degree of mixing between the originally rather segregated components may be a hard task or, depending on the space and time scales of the mixing process, a complete mixing may even be impossible without special mixing devices. For instance, specially designed spacers in the nuclear fuel are needed to enhance the turbulent heat transport, and mixers are used to avoid thermal fatigue due to temperature fluctuations when flows with different temperatures meet within a tee-junction.

All these situations rely on turbulent mixing that, according to Dimotakis (2005), “can be viewed as a three-stage process of entrainment, dispersion (or stirring), and diffusion, spanning the full spectrum of space-time scales of the flow”. The mixing level, or quality of mixing, may be estimated, according to Brodkey (1967), through two parameters. The first parameter is the scale of segregation that gives a measure of the size of the unmixed lumps of the original components, i.e. a measure of the spreading of one component within the other. A length scale or a volume scale, analogous to the integral scales of turbulence, may be defined based on the Eulerian autocorrelation function of the concentration. Since the scale of segregation provides a measure of the extent of the region over which concentrations are appreciably correlated, it constitutes a good assess of the large-scale (turbulence-controlled eddy break-up) process, but not of the small scale (diffusion-controlled) process. The second is the intensity of segregation, given by the one-point concentration variance normalised with its initial value. It constitutes a measure of the concentration difference between neighbouring lumps of fluid, i.e. it describes the effect of molecular diffusion on the mixing process.

But, according to Kukukova et al. (2009), a general, objective and complete definition of mixing, or of its opposite, segregation, needs a third parameter, or dimension, as the authors of the reference express it, namely the exposure or the potential to reduce segregation. This rate of change of segregation associated to a time scale of mixing, combines the strength of the interaction, in this case the turbulent diffusivity, the concentration gradients and the contact area between components. Therefore, good mixing characterized by a small scale of segregation and a low intensity of segregation may be achieved if the mixing process is contained within the exposure time scale, i.e. for adequately high exposure.

However, many design problems of light water reactors that have arisen during their operation, originate from overconfidence about the mixing properties of turbulence. A classic example is that of the mixing of feedwater and reactor water in the downcomer of a BWR, in connection with Hydrogen Water Chemistry (HWC) to mitigate Intergranular Stress Corrosion Cracking (IGSCC) of sensitized stainless steel. The injection of reducing hydrogen gas to the feedwater was intended for recombination with oxidizing radicals contained in the reactor water and produced by radiolysis, through a turbulence-induced, optimal mixing in the downcomer. Surprisingly, the recombination effect for Units 1 and 2 of Forsmark NPP was not in proportion to the amount of injected hydrogen and the only solution appeared to be a major increase in the addition rate of hydrogen. But, in 1992, a very primitive and

rough CFD model of an octant (45°) of the downcomer (Hemström et al., 1992) indicated that the flow field and the mixing were rather complex and highly three-dimensional, leaving the regions between feedwater spargers with practically no mixing, and that buoyancy ostensibly aggravated the mixing issue. The poor mixing in the downcomer of Units 1 and 2 of Forsmark NPP arose from the design of the core shroud cover that, radially and freely over its entire perimeter, directed the warmer reactor water coming from the steam separators into the downcomer. Owing to the limited azimuthal extent of the four feedwater spargers, four vertical regions without direct injection of colder feedwater were established in the downcomer. Due to buoyancy combined with mass conservation, the colder and falling regions contracted azimuthally, making the warmer and slower regions to expand. Turbulence acted within the colder regions, tending rather effectively to achieve temperature homogeneity, and at the boundary areas between the warmer and colder regions. The transit time of the vertical flow in the downcomer was not long enough for turbulence to achieve a complete temperature homogenization of the recirculation water. In other words, the turbulent diffusivity, the temperature gradients and the contact surfaces between cold and warm water were not large enough to achieve a good mixing, i.e. the exposure was too low. The mixing was achieved further downstream in two main steps, namely by forcing cold and warm water to meet within the inlet pumps, at the bottom of the downcomer, and by rotating agitation within the remnant vortices at the pump outlets, produced by the Main Recirculation Pumps (MRP). This mixing process is quite effective, leaving only less than 3 % difference in temperature (Tinoco and Ahlinder, 2009) but for HWC, this homogeneity comes too late in the process since radiation at the level of the core in the downcomer is needed for triggering recombination of oxygen with hydrogen.

Finally, the problem of poor mixing in the downcomer was significantly reduced by modifying the design of the core shroud cover. Cylindrical-vertical walls were placed at the edge of the cover in the azimuthal locations facing the regions between spargers in order to completely block the reactor water flow. Radial flow out of the cover was allowed only regions in front of the spargers. This design was first tested in a rather advanced CFD model (Ahlinder et al., 2007), used to investigate HWC. The results obtained showed a higher degree of recombination with the modified core shroud. However, the decisive factor in the recombination was the level of radiation absorbed by the water in the downcomer, indicating that an effective recombination might not be possible over the complete fuel cycle without a modified core design. For a couple of years ago, this shroud cover design was implemented in Units 1 and 2 of Forsmark NPP, as a step in the modernisation and improvement of the process and safety to cope with a programmed power uprate. HWC was not carried out due to the aforementioned core design issue but an improved mixing in the downcomer has other advantages like minimizing the risk of cavitation in the MRPs.

The most complete CFD model including for the first time rotating MRPs was developed in 2008 (Tinoco and Ahlinder, 2009) for studying thermal mixing in an internal pump BWR. Figure 5 shows in (a) once more the view of the reactor as a reference, and in (b) it shows a view of the geometry involved in the CFD model that is limited from above by the free water surface. The model includes the downcomer (the water annular region between the inner

surface of the reactor and the outer surface of the core shroud), the MRPs (4 pumps for this half of the reactor) and the lower plenum with the guide tubes of the control rods which extend to the entrance of the core reactor. In (c) a MRP is shown in more detail and in (d) the lower plenum, also in more detail. The complete CFD model contains slightly more than 25 million cells to represent the included part of the reactor. The correct flow through the model is achieved by rotating the pumps to the adequate rotational speed for normal operation. The thermodynamic properties of water as a function of pressure and temperature have been included in the physical properties of the studied fluid, allowing with that the analysis of the mixing of warmer recirculation water with cooler feed water. The results indicate a substantial mixing at the lower plenum inlet, being the maximum difference in the temperature of water entering the reactor core of about 2.5 °C (see Tinoco and Ahlinder, 2009). This model may be used in the future to analyse the mixing of boron injected to the reactor with the surrounding water, as suggested below.

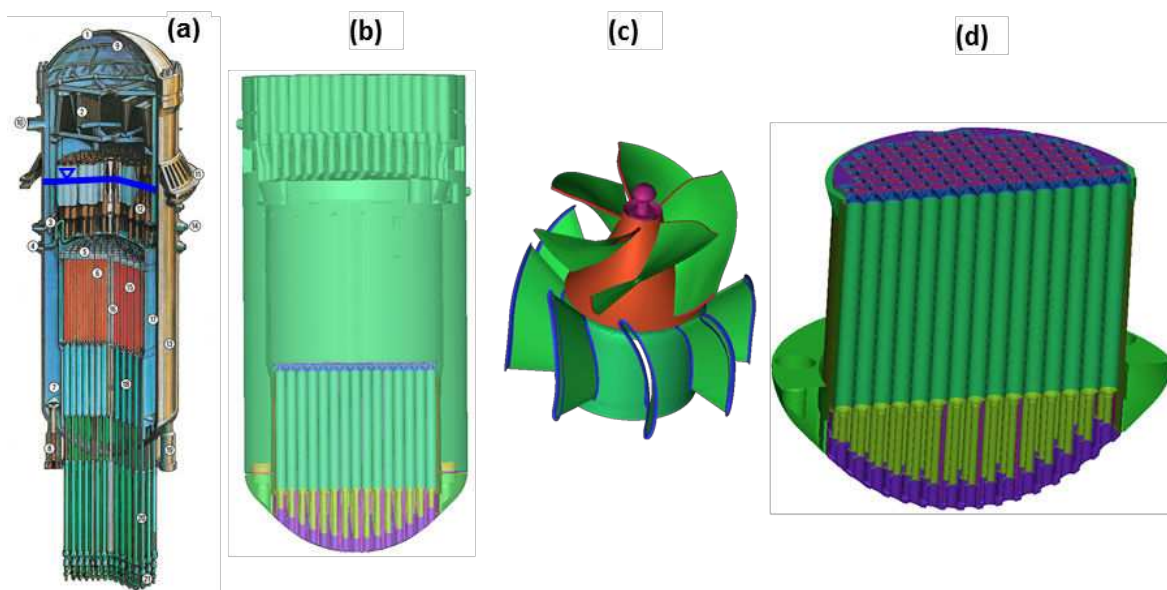


Figure 5. (a) View of the reactor; (b) Model of the Downcomer, MR Pumps and Lower Plenum limited from above by the free water surface; (c) Model of MR Pump with diffuser vanes; (d) Lower Plenum detail with control rod guide tubes.

Originally, this CFD model consisted of two separated sub-models linked by boundary conditions at a common surface constituted by the Lower Plenum Inlet, since this split was geometrically and computationally optimal. The Lower Plenum Inlet is constituted by cylindrical-rectangular openings located almost directly downstream of the MRP outlets equipped with diffuser vanes. Even if these diffuser vanes recover an important amount of the mechanical energy stored in the rotation of the flow imparted by the pump, a vortex is still formed with a significant downstream extension, being this vortex responsible for an appreciable part of the thermal mixing. The use of a surface, as outlet for the first sub-model and as inlet for the second sub-model, to transfer the information of the flow behaviour from one sub-model to the other is not adequate. The information corresponding to the dif-

ferent fields is correctly transferred but no information about the field tendencies, i.e. the different gradients, reaches the second sub-model. In this case, the further development of the vortices coming from the pumps is corrupted beyond the inlets of the second sub-model. The result is a rather strong underestimation of the thermal mixing, predicting temperature differences of the order of 10 %, (see Tinoco and Ahlinder, 2009), temperature differences that have never been detected by measurements or, indirectly, by contingent fuel damage. The analysis of the different turbulence parameters objectively endorses this difference in mixing, which leads to the only reasonable recommendation of using a larger and computationally heavier model but right from the point of view of the physics of the flow. Model separations in CFD simulations, similar to the one described above, will deliver proper results only if the different gradients associated with the flow are small or negligible, otherwise a finite, common, transition volume is needed. This type of coupling between two CFD models might be difficult to achieve in rather standard commercial codes.

By Regulatory compliance, the safety system for the injection of boron to achieve an emergency stop of the reactor in case of an ATWS is now automatically operated in Units 1 and 2. Due to the automation, the accidental or programmed injection of boron will be associated with a set of new cases of postulated accidents that have to be analysed. Since the injection of boron in these Units is done in only two points, closely and not symmetrically located in the upper downcomer, the probability of an inhomogeneous distribution of boron, especially at the entrance of the core, is very high, as a preliminary study using a reduced model containing only the downcomer indicates (Tinoco et al., 2010a). This situation may lead to rapid variations in space and time of the reactivity of the core that might result in local maxima of thermal power that could ultimately damage the fuel and/or adjacent structures. The CFD simulations of boron injection and its mixing with the reactor water have to be linked to three-dimensional simulations of the neutron kinetics of the reactor core in order to correctly capture the physics of these thermal power variations.

5. Heat transfer

Turbulent thermal mixing implies, of course, transfer of heat from the warmer component, or fluid, to the colder component, resulting in a tendency to temperature and enthalpy homogenization. But, depending on the geometry of the thermal system, the process towards homogenization may have a rather well defined composition that involves the system boundaries which, in general, correspond to solid structures. These structures interact thermally with the fluid or fluids involved in the thermal mixing process, being the composition of the process decisive for the behaviour of the structures. According to the viewpoint of this work, the composition of the thermal mixing process includes firstly the morphology of the turbulent flow involved, i.e. the flow geometry, the eddy structure, the presence of stable boundary layers, etc. Secondly, it includes the thermophysical properties of the fluid and the thermophysical and geometrical properties of the solid boundaries. Depending on the composition of the thermal mixing process, the solid boundaries may or may not be exposed to the problem of high-cycle thermal fati-

gue. Therefore, the composition of the thermal mixing process, as defined above, implies the analysis of the complete system, including the solid boundaries, i.e. the type of heat transfer which is denoted as conjugate heat transfer, with rather advanced requirements regarding comprehensive information of the turbulent flow involved. The aforementioned concepts discussed so far will be emphasized through a slightly different analysis of the paradigm of thermal mixing and fatigue, i.e. the tee-junction.

5.1. Thermal mixing in a tee-junction

This exemplar of thermal mixing has been and is still being extensively studied, both experimentally and numerically, as the work of Naik-Nimbalkar et al. (2010) confirms with a rather wide, but not absolutely comprehensive, review of the literature about the subject. Probably the review should be completed by mentioning the experimental work of Hosseini et al. (2008) about the classification of the branch jet flow and about the structure of the flow field (Hosseini et al., 2009). Also other publications not included in the aforementioned review, (Muramatsu, 2003, Ogawa et al., 2005, Westin et al., 2008, OECD/NEA, 2011), that are experimental or including an experimental part for validation of a numerical simulation, investigate the bulk flow structures of the mixing in a tee-junction. All the references mentioned in this Subsection, and many others not included due to lack of space, have, as the main motivation, the purpose of studying, understanding and eventually controlling the wall temperature fluctuations associated with thermal fatigue. Particularly the reference OECD/NEA (2011), which is a rather major effort to validate numerical simulations of the thermal mixing in a tee-junction, clearly proclaims: “In T-junctions, where hot and cold streams join and mix (though often not completely), significant temperature fluctuations can be created near the walls. The *wall temperature fluctuations* can cause cyclical thermal stresses which may induce *fatigue cracking*”. But none of these references presents temperature or velocity data of the wall near region, i.e. the boundary layers, or of temperature at the walls. Even worse, the solid walls are never involved in any measurements, although it is the propagation of temperature fluctuations from the surface and inside the solid that may lead to fatigue cracking.

The reason for the absence of this crucial part of the mixing matter may be the great difficulty in measuring very close to walls and within the walls. For instance, velocity measurements in a thin boundary layer with Laser Doppler Velocimetry (LDV) are biased by even small density differences in the fluid, and temperature measurements within the solid are intrusive, cannot be relocated and may lead to errors due to contact continuity. But, in situations when temperature may be considered as a passive scalar, i.e. relatively small temperature differences not affecting the flow, the velocity measurements may be carried out in isothermal conditions. Since measurements of this kind have been done in this and other situations, to be reported in what follows, the true reason for the absence of this type of measurements in the study of tee-junction flows may be lack of knowledge about how vital the information related to temperature fluctuations close to the wall and within the wall is for understanding and being able to estimate the risk for wall thermal fatigue in a specific case. Of course, the information about flow behaviour close to the wall is directly related to the

behaviour of the flow in the bulk, but the physical properties of fluid and the physical and geometrical properties of the wall will also affect the near wall flow, as the next paragraphs of this Subsection will describe. In other words, the problem of turbulent thermal mixing in a tee-junction is a process with a well-defined composition that has to be solved in its wholeness, i.e. a conjugate heat transfer problem.

As the preceding discussion reveals, measurements of the temperature fluctuations due to heat transfer within the boundary layer of a fluid close a wall and/or within the solid wall are very scarce. The work of de Tilly et al., (2006), de Tilly and Sousa (2008a) and de Tilly and Sousa (2008b) deals with the development of a multi-thermocouple planar probe of dimensions of the order of 300 μm to measure the instantaneous values of the wall heat flux in a boundary layer. Preliminary results of the wall heat flux have been obtained for the boundary layer flow developing downstream of a two-dimensional tee-junction. Even if this device is very promising, some questions arise from these tests, namely how to check the accuracy of the measurements with an independent method, how to handle thinner boundary layers than the instrument and how to deal with three-dimensional flow. In any event, this novel concept deserves a positive and successful development as a significant contribution to a difficult but important subject.

The measurements reported by Mosyak et al. (2001) seem to move this discussion away from the trail of wall temperature fluctuations and the risk of fatigue cracking since this reference treats the subject of constant heat flux boundary condition in heat transfer from the solid walls of channel flow. However, the experimental data substantiate the analytically demonstrated fact (Polyakov, 1974) that temperature fluctuations near a wall differ for different combinations of fluid and solid in conjugate heat transfer problems. Also Direct Numerical Simulations (DNS) of conjugate heat transfer (Tiselj et al., 2001, Tiselj et al., 2004, Tiselj, 2011) corroborate this information, where the governing parameters of the fluid-solid combination are the wall thickness d_w , the thermal activity ratio $K = \sqrt{(\rho \cdot c_p \cdot \lambda)_f / (\rho \cdot c_p \cdot \lambda)_w}$ and the ratio of thermal diffusivities $G = \alpha_f / \alpha_w$. Here, ρ is the density, c_p the isobaric specific heat, λ the thermal conductivity and $\alpha = \lambda / (\rho \cdot c_p)$ the thermal diffusivity. The sub-indices f and w indicate respectively "fluid" and "wall". Depending on the values of d_w and K , two asymptotic limits of the conjugate turbulent heat transfer exist at the same Reynolds and Prandtl numbers and at the same wall heat flux. When $K \rightarrow 0$ and $d_w > 0$, the turbulent temperature fluctuations do not penetrate the wall and the wall temperature does not fluctuate. When $K \rightarrow \infty$, d_w is of no importance, the turbulent temperature fluctuations do penetrate the wall and the wall temperature does fluctuate. In a particular solid-fluid case with given K and d_w , the wall temperature behaviour will be between these two limiting cases, as may be observed through the results of Tiselj et al. (2001), given in Figure 6.

The results displayed in Figure 6 are not completely general since they have been obtained for $G=1$, as Tiselj and Cizelj (2012) point out, while $\text{Pr} \approx 0.9$, $K \approx 0.2$ and $G \approx 0.04$ for water and stainless steel at the pressure and temperature conditions of a BWR. Nonetheless, the main conclusion of these results is that, despite the large spectrum of temperature fluctua-

tion variations as functions of the aforementioned material and geometrical parameters, the heat transfer rate for the limiting case $K = \infty$ is only 1 % higher than that for the other limiting case $K = 0$. The reason for this coincidence is the fact that the heat transfer rate is associated with the mean temperature gradient, which is very similar in both cases. These are good news for the heat exchanger designers, but the large spectrum of temperature fluctuation variations is bad news for the nuclear and other designers responsible for the mechanical integrity of solid structures.

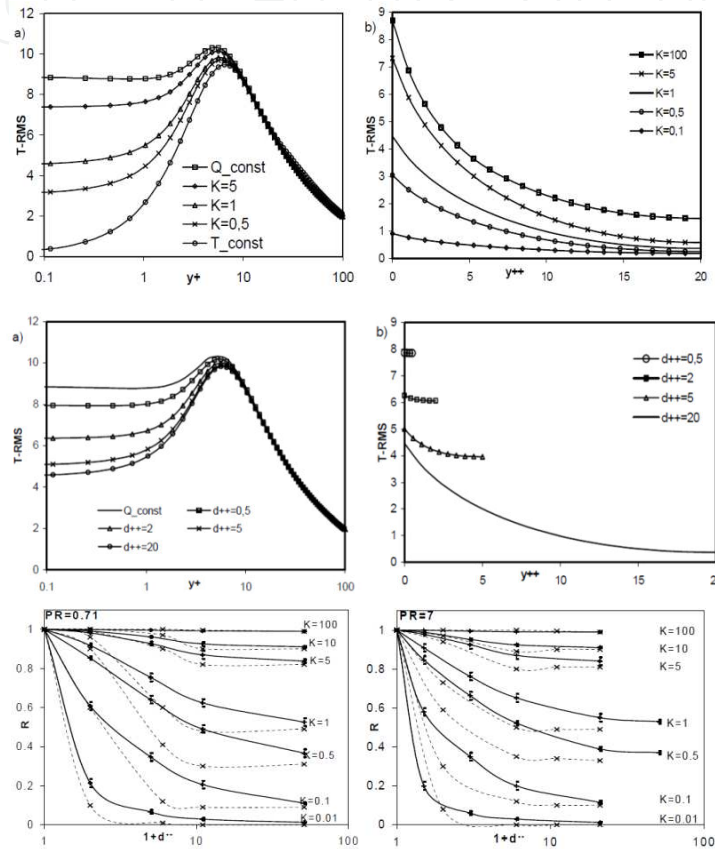


Figure 6. Temperature fluctuations from Tiselj et al. (2001) with ASME permission. Upper view: RMS-values, $Pr = 7$, $d^{++} = 20$, (a) fluid; (b) solid. Middle view: RMS-values, $Pr = 7$, $K = 1$, (a) fluid; (b) solid. Lower view: RMS-values normalized with ideal RMS-value of $K = \infty$, (a) $Pr = 0.71$; (b) $Pr = 7$; dotted lines from Kasagi, N., Kuroda, A., and Hirata, M., (1989).

The value $G=1$ associated with the results of Tiselj et al. (2001) shown in Figure 6, implies that the scale $y^{++} \equiv y^+$, $d^{++} \equiv d^+$ since $y^{++} = \sqrt{G}y^+$, a scale used for the results of Figure 6. Tiselj and Cizelj (2012) mention that this scale has an uncertain meaning and should be abandoned. Also, smaller values than $G=1$ will probably lead to lower temperature fluctuations inside the wall, as the results of Tiselj and Cizelj (2012) indicate, but for $Pr=0.01$. According to Figure 6, an increase in the Prandtl number will further decrease, though moderately, the temperature fluctuations inside the wall. The conclusion of Tiselj and Cizelj (2012) is that, for the combination liquid sodium-stainless steel ($K \approx 1$, $G \approx 10$), the results indicate a relative high penetration of turbulent temperature fluctuations into the simulated heated wall.

The lower values of the parameters for the combination water-stainless steel of BWR suggest that the penetration of turbulent temperature fluctuations in walls will be rather low under the conditions investigated through DNS simulations of channel flow. But, in other circumstances such as tee-junctions or control rod stems, which will be discussed in the next Subsection, the temperature fluctuations seem to be large enough to cause damage through thermal fatigue. It seems apparent that further investigation is needed to elucidate the wall behaviour in cases where no stable boundary layers are built and large structures coming from the bulk flow may strongly interact thermally with the walls. A first step in this direction has been taken by van Haren (2011), where a DNS of a tee-junction has been carried out. Unfortunately, only very preliminary results have been reported since, due to high computer requirements, the run-time was not enough to obtain a statistically stationary and converged solution.

Hopefully, the preceding discussion has made clear that the problem of thermal fatigue induced by flow temperature fluctuations is a conjugate heat transfer problem, i.e. a heat transfer problem of the specific combination fluid-wall. More knowledge is needed to understand the aforementioned interaction between large structures generated in the bulk flow and the walls. This knowledge should be obtained primarily by experiments but further difficulties with temperature measurements should be added to those already mentioned, i.e. intrusive, non-relocatable and contact continuity problems. For instance, the specificity of the combination fluid-wall questions the use in an experimental facility of Plexiglas or other material than the precise of the prototype to be investigated. Even the conditions of the experiment should match those of the prototype since they affect the different material parameters that ultimately influence the thermal fluctuations. Intrusive measurements have to be done with material properties matching those already mentioned of the walls, not only thermal conductivity. For instance, at the FATHERINO 2 facility at CEA Cadarache, briefly described by Kuhn et al. (2010), a thin brass mock-up ("Skin of Fluid Mock-up") has been developed to visualize, by infrared thermography, the mean and fluctuating temperature fields at the interface of the fluid and the wall. This mock-up may only have relevance as a case for validating numerical simulations, as it is used by Kuhn et al. (2010), but more knowledge is needed about the correct conditions, to be discussed below, for simulating the wall heat transfer, including the right distribution of temperature fluctuations within the wall.

Numerical simulations of conjugate heat transfer including temperature fluctuations inside the solid structure other than DNS have already been carried out using diverse approaches. The previously mentioned reference, Kuhn et al. (2010), uses a LES approach to resolve the flow and temperature fields inside the fluid for two cases, namely a thin-wall brass model and a thick-wall steel model. The results show relatively large differences between models in both the mean temperature fields and the distribution of temperature fluctuations inside the solids. This is attributed only to the heat conduction in the thicker wall, apparently both radial and axial, with no further analysis of other possible reasons, i.e. nothing is commented about the different combinations fluid-solid. From the numerical point of view several questions arise, firstly the fact that the same grid is used for the two walls. Secondly, y^+ may

be up to 5 in the mixing region when requirements in LES of channel flow, for less than 1 % difference in heat transfer rate with DNS results, are $y^+ = 0.5$, $x^+ = 30$ (streamwise) and $z^+ = 10$ (spanwise), according to Carlsson and Veber (2010). In Kuhn et al. (2010) nothing is mentioned about the grid resolution in the streamwise and/or spanwise directions. However, a validation like that of Carlsson and Veber (2010) about the distribution of temperature fluctuations has not yet been carried out, a situation that sheds some doubts about the accuracy of the results obtained in Kuhn et al. (2010) and, for the rest, of the results obtained with any other methods different from DNS.

A brief and definitely incomplete review of other approaches reveals the use of LES with thermal wall functions (Châtelain et al., 2003). The results show that the temperature fluctuations in the vicinity of the wall and inside the wall can be highly underestimated a fact that is corroborated by Pasutto et al. (2006) and Jayaraju et al. (2010). Also some attempts have been done with the RANS approach, with varied results (Keshmiri, 2006, Tinoco and Lindqvist, 2009, Tinoco et al., 2010b, Craft et al., 2010), and with the more unconventional Lagrangian approach of Pozorski and Minier (2005). The majority of the numerical results discussed in this Subsection are waiting for an experimental validation, or numerical by DNS, in order to be able to establish the correct methodology to be used in future simulations for estimating the risk of thermal fatigue.

5.2. The control rod issue

Broken control rods and rods with cracks were found in the twin reactors Oskarshamn 3 and Forsmark 3 in the fall of 2008. As a part of an extensive damage investigation, time dependent CFD simulations of the flow and the heat transfer in the annular region formed by the guide tube and control rod stem were carried out with a model containing 9 million computational cells (Tinoco and Lindqvist, 2009). Due to limitations in time and computer resources, only a quadrant of the guide tube and control rod with an axial length of approximately 1 m was included in the model, as Figure 7 shows. Also an Unsteady RANS (URANS) approach with the SST $k-\omega$ model was chosen for handling turbulence.

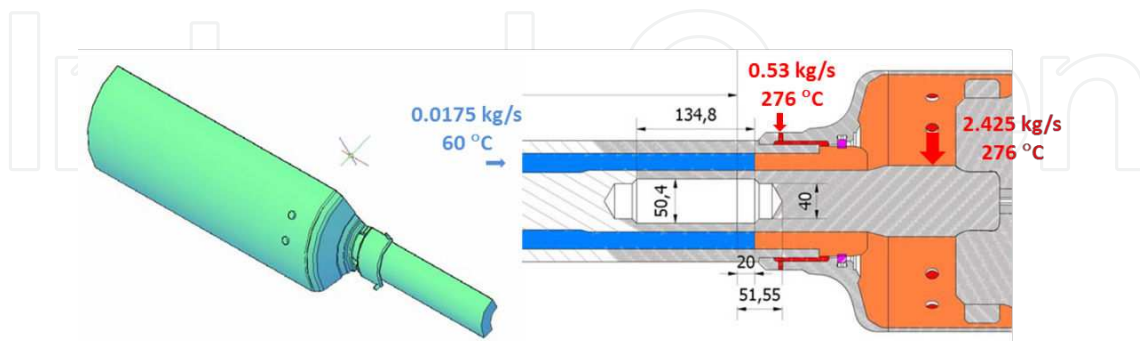


Figure 7. CAD view (left) and drawing of a part of the CFD model used in Tinoco and Lindqvist (2009).

In this figure, where gravity is from right to left in the right view, the different mass flow rates per quadrant are indicated with their temperatures by arrows. The upper bypass inlet (right) divides its mass flow rate into two holes of 14.6 mm in diameter, resulting in inlet ve-

locities of about 10 m/s. The lower bypass inlet has only one hole of 8 mm in diameter that connects to an annular channel before the flow is delivered with relatively low velocity to the annular region between control rod stem and guide tube.

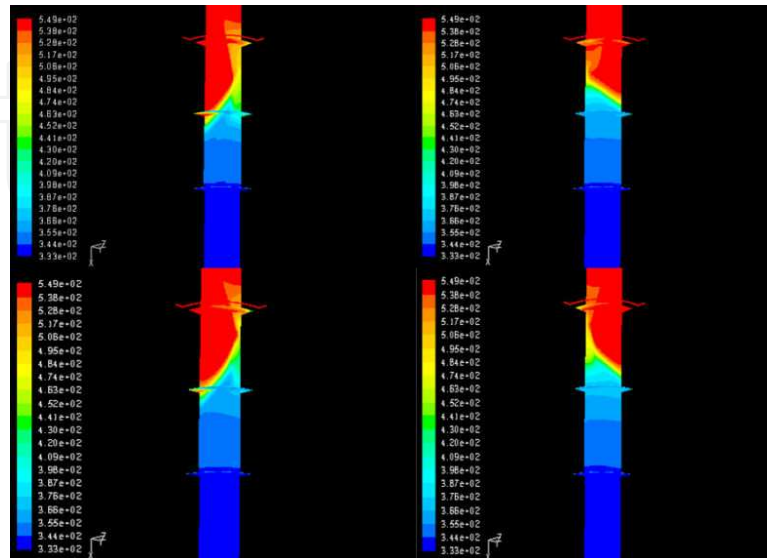


Figure 8. Temperature sequence showing a large scale variation of the surface temperature of the control rod stem with a period of ~15 seconds (temperatures in K).

Figure 8 shows a typical time sequence, from left to right and in two rows, of the surface temperature of the control rod stem with a large scale variation with a frequency of approximately 0.07 Hz. Three horizontal planes are shown in the views, namely the upper plane corresponding to the lower bypass inlet, the middle plane corresponding approximately to the region of the break (10 cm below the lower bypass inlet) and the lower plane corresponding approximately to the end of the inlet region of the cold crud-cleaning flow (20 cm below the lower bypass inlet). These simulations together with metallurgical and structural analyses indicated that the cracks were initiated by thermal fatigue.

The results of the damage investigation were accepted by the Swedish Nuclear Regulatory Authorities for a reactor restart with new control rods. Meanwhile, further studies had to be accomplished to clarify some remaining matters. One of the contested issues concerned the validity and accuracy of the CFD simulations. Consequently, new CFD models, (Tinoco et al., 2010b), were developed in conformity with the guidelines of Casey and Wintergerste (2000) and Menter (2002), while the URANS approach with the SST $k-\omega$ model was preserved, and validation experiments were carried out. The largest CFD model contained 16.8 million cells because large effort was put into maintaining a value of $y^+ \sim 1$ for the dynamic mesh resolution in the near wall region of the control rod stem at the level of the mixing area. Validation tests had indicated that a y^+ close to 1 is a necessary condition to ensure sufficiently accurate heat transfer results (Tinoco et al., 2010b), but no control was done about the values of x^+ and z^+ since the results of Carlsson and Veber (2010) were at that time not

known. Figure 9 shows the low y^+ values for the grid at the stem wall in the mixing region indicated by the horizontal black line for different times of the simulation.

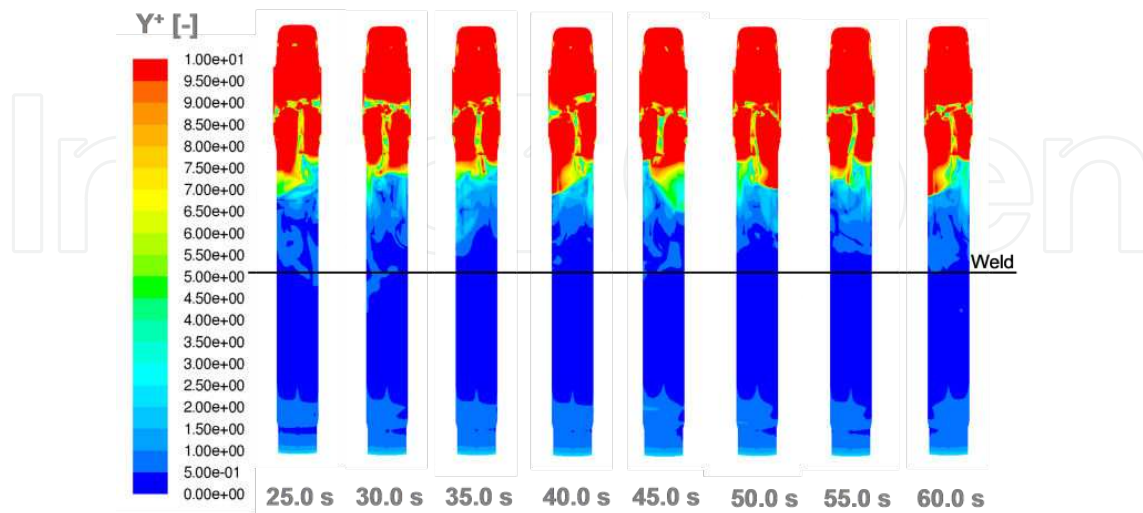


Figure 9. Grid y^+ adjacent to the control rod wall at different times of the simulation.

Figure 10 shows in the upper view a sequence of colour pictures representing the velocity magnitude, maximized to 1 m/s (red scale ≥ 1 m/s), in a vertical plane bisecting the quadrant and containing the region below the jets of the upper bypass inlet. The pictures are completely symmetric since the original data of the quadrant have been mirrored with respect to vertical axis. In this sequence, it is possible to observe many structures forming and moving downwards, towards the lower bypass inlet, in the annular region between the stem and the guide tube. In this view, the black line indicating the level of the stem weld corresponds to the level of plane 7 shown in the middle view.

The middle view depicts five time signals of the axial vertical velocity component of the fluid at radially 2 mm from the stem wall. The points are located in plane 7 (blue line in left reference picture) at 5 different azimuthal positions. The signals indicate large vertical intermittent movements downwards, with speeds of the order of 1 m/s and frequencies of 0.1-0.2 Hz which corroborate the impression given by the pictures of the upper view. This is the dynamical mechanism of the mixing responsible for the thermal fatigue of the control rod stems. This effect has been further confirmed by simulations of guide tubes without the upper bypass inlet, reported in Tinoco and Lindqvist (2009), where no such structures are present.

The lower view shows the thermal consequences of the above described dynamical process that transports large lumps of warm fluid downwards with relatively large velocities. The maxima of the temperature time signal correlate well with the minima of the axial vertical velocity component. The fact that the temperature signal (in blue) corresponds to only one single fluid point indicates that the lumps of warm fluid cover a large part of the annular gap modelled in the quadrant. This view also shows the temperature signal of two points located inside the solid, namely the first located radially at 0.5 mm from the stem outer wall

(in green) and the second located radially at 2 mm from the wall (in red). In this graph, it is possible to observe that, compared to the fluid signal, both solid signals are damped, with high frequency variations filtered out. Also, the red signal is not always smaller than the green indicating switches in the direction of the heat flux.

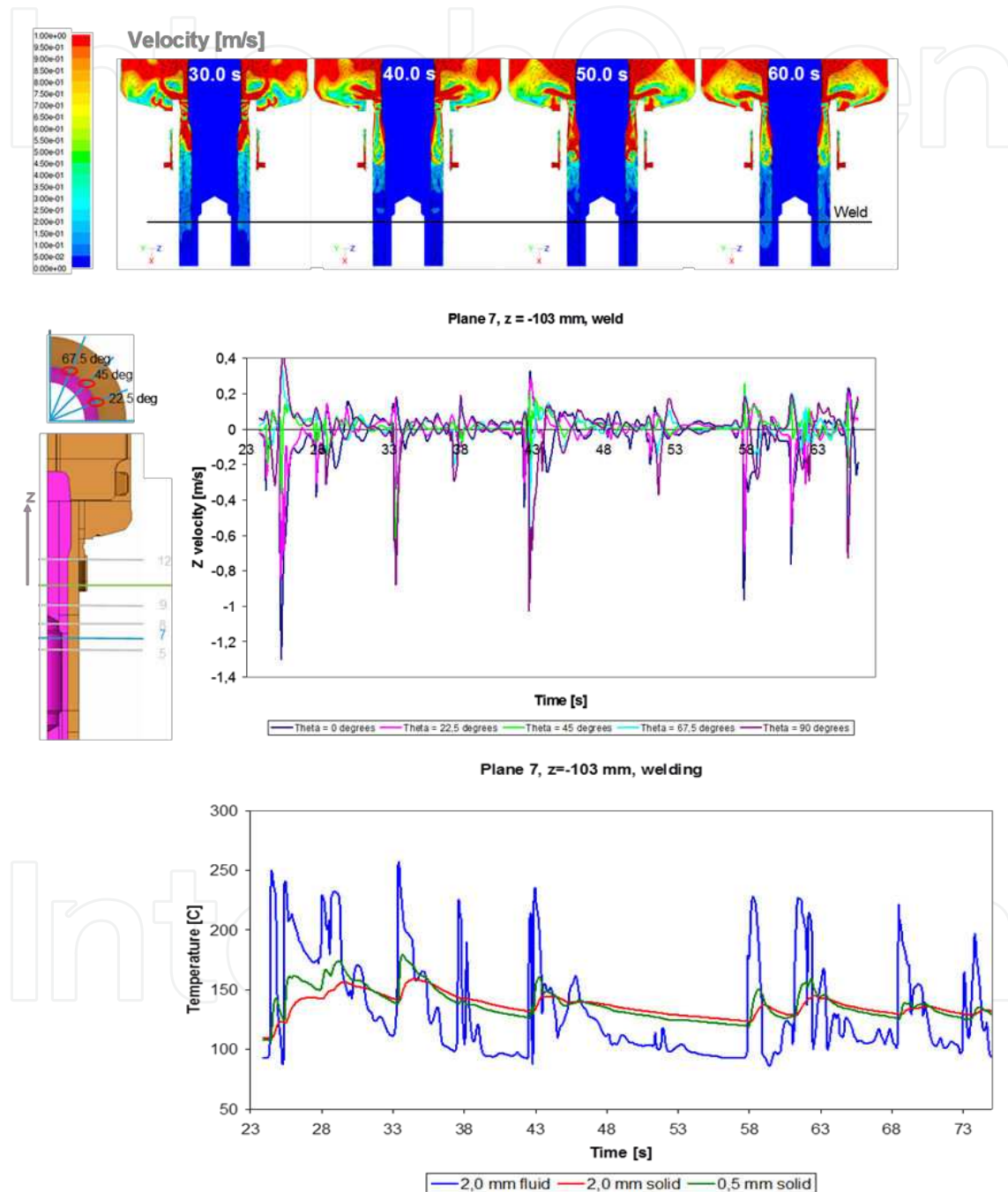


Figure 10. Upper view: velocity magnitude limited to 1 m/s (red \geq 1 m/s). Middle view: time signal of axial vertical velocity component of the fluid in plane 7 (blue line in left reference picture) at 2 mm from the stem wall and for 5 different azimuthal positions. Lower view: temperature signal at three radial points at plane 7 with azimuthal angle of 45°.

However, the central question is still the quality of these simulations. Is a URANS simulation with good spatial and time resolutions enough to capture both the flow field and the heat transfer correctly? The author is tempted to answer with a “yes” but a more objective answer should be “probably”. If the resolutions are adequate, the URANS approach based on SST $k-\omega$ model seems to work properly for cases with high enough Reynolds numbers and turbulent flow containing large perturbations. Furthermore, the comparison with experiments shown in Figure 11 exhibits a rather good agreement for mean temperature and temperature fluctuation distributions along a vertical line 1 mm apart from the stem wall. Incidentally, the material properties in the experiment are those of the prototype. Unfortunately, no comparisons of the velocity and velocity fluctuation fields were done but it is difficult to think that the agreement in the temperature fields shown in Figure 11 may be achieved with a radically different velocity field to that of the experiments.

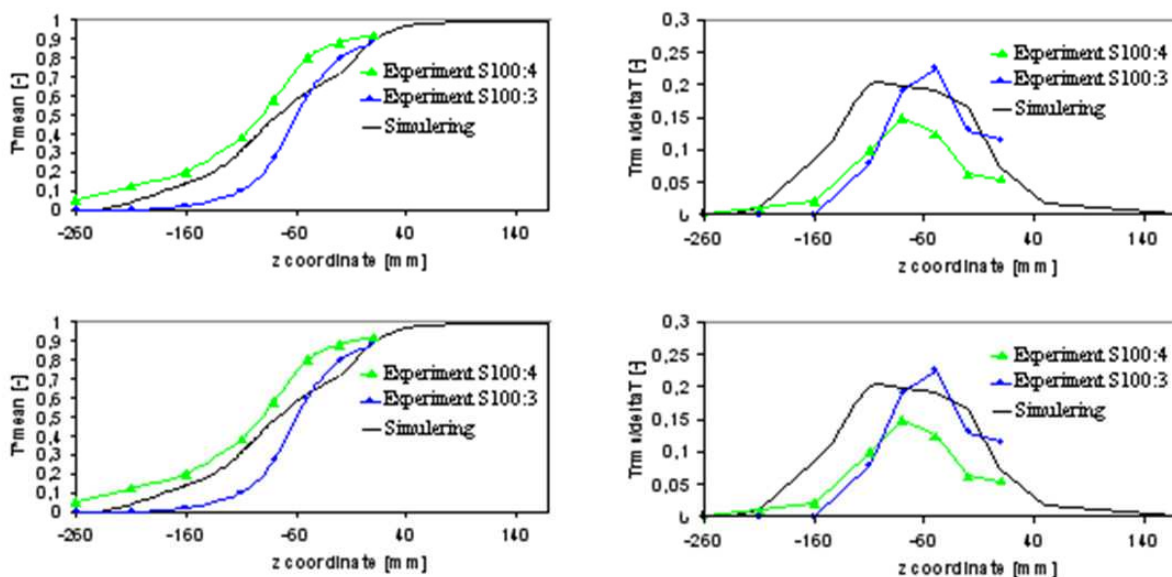


Figure 11. Comparison with the steel model experimental data (see Angele et al., 2011); left: mean temperature; right: temperature fluctuations (rms-value).

Then, are the simulated temperature fluctuations inside the solid stem also correct? This question is more difficult to answer since no experimental validation has been carried out but indirect indications about some properties of these fluctuations have nonetheless been obtained. Some of these properties are the order of magnitude of the most energy-containing frequencies of the temperature fluctuations at stem wall and of the associated heat transfer coefficients. Structural analyses (see e.g. Forsmarks Kraftgrupp, 2009) using this range of frequencies, together with the large temperature amplitudes and velocities of the order of 1 m/s, show that this kind of heat transfer is associated with the initiation of cracks on the stem surface. Moreover, the analyses also show that the time scale of the crack development that resulted in broken control rod stems is consistent both with the geometry of the stem (hollow welded joining; see Tinoco and Lindqvist, 2009) and the thermal loadings arising from the heat transfer process described by the CFD simulations. In general, the re-

sults of the structural analyses based on the aforementioned CFD-simulated conditions are consistent with the damage picture obtained by inspection. Using more “conservative” conditions, e.g. higher heat transfer coefficients, leads to unrealistic short time scales of the damage.

Furthermore, the mathematical and physical consistency of the temperature field inside the stem has been demonstrated by solving of the Inverse Heat Conduction Problem (IHCP), (Taler et al., 2011). The IHCP is defined as the determination of the boundary conditions of the problem from transient temperature histories given at one or more interior locations. The IHCP is a so called ill-posed problem, i.e. any small change on the input data can result in a dramatic change of the solution. By giving CFD-computed time signals of the temperature at selected points inside the stem, the temperature signal and the heat flux at the surface of the stem were recovered with good accuracy. The question that remains is the correctness of the temperature fluctuations at the surface of the stem, i.e. the correctness of the thermal interaction between the solid surface and the near wall region of the fluid. A definite answer can only be obtained by experimental validation or DNS.

Summing up, further structural analyses based on the same CFD-computed conditions have led to a set of measures that have been taken and/or are being implemented. The crud-cleaning flow has been modified to deliver a flow with a temperature of up to 100 °C instead of the original of 60 °C. After turning, a control rod stem may acquire surface tensile residual stress which increases the risk of crack initiation. In order to counteract this undesirable effect, all control rod stems are now burnished since this procedure creates surface compressive residual stress that increases the resistance of the stem against damage, i.e. increased protection against crack initiation and crack growth. At locations of the core most exposed to high warm bypass flows, a better material, stainless steel XM-19, has been chosen for the stems of the control rods. Only 50 of the 169 control rods will keep stems of a somewhat poorer material, stainless steel 316L. In the fuel outage of year 2014, all control rods will be tested in order to detect the presence of cracks and, based on the existent experience at that time, a renewed test program will be decided. This set of measures has been conceived as a viable alternative to the very expensive option of eliminating the cause of the mixing problem by changing the design of the control rod guide tubes comprising a new location of the upper bypass inlet.

6. Conclusion

This chapter constitutes a partial view of CFD, both in the sense of limited and favouring, since, for instance, the examples concerning BWR applications are overrepresented and important subjects such as nuclear safety and two-phase flows are left aside. As a kind of defence, it may be argued that the methods used for BWRs are valid, in general, for PWRs and, probably with important modifications, for SuperCritical Water Reactors (SCWRs). As far as CFD in nuclear safety is concerned, the high interest and large amount of work in the subject from, among others, the European Commission, (European Commission, 2005), and the U.S.

Department of Energy, Idaho National Laboratory, (Johnson et al., 2006), make an analysis and a review of the subject rather superfluous.

As pointed out by Tinoco et al. (2010c), two-phase flow simulations still have a relatively high degree of uncertainty and they have not reached the level of quality of single-phase simulations. The physics involved in two-phase phenomena is still not well understood, due mainly to the measuring difficulties entailed by the requirement of local knowledge of the processes needed in CFD. Consequently, the models available lack the distinctive prediction capability of CFD because they are usually based on information collected as relatively general correlations. A fundamental example is the experimental lack of knowledge about the modification by boiling of the detailed structure of a boundary layer at a wall. This deficiency leads to wrong predictions of flow resistance and void distribution in, for instance, pipe flow with boiling from the walls.

Another topic that has not been mentioned in this work is the field of acoustic perturbations in the reactor system, especially in the parts corresponding to pipe networks. The problem of flow-induced structural resonances has become more topical due to the increased interest in operating the reactors at uprated power output. The new components and/or the increased flow rates necessary for achieving the upgrade may lead to the generation of pressure waves that may excite structural vibration modes and increase the risk of mechanical fatigue. CFD may be used to analyse the pipe-network system if the geometry is realistically represented, the grid has a suitable resolution, the turbulence model is appropriate and, in the case of steam, compressibility is included (Lirvat et al., 2012). Post-processing of the generated data can provide information about the flow induced excitation modes, the source of the excitation frequencies/modes and possible standing pressure waves. In the past, attempts have been carried out to collect acoustic signals generated in complex systems like a nuclear reactor in order to detect possible deviations from normal operation of the different components. Any success has failed to turn up not due to the process of acquiring the data, which is relatively easy, but to the difficulties in interpreting the signal constituted by the superposition of broadcasted pressure waves from every component that may act as a source. In the future, CFD might help identifying the sources and describing how the different pressure waves propagate in the system. Perhaps, detecting the leakage of valves in complex systems like a nuclear reactor by means of acoustic signals may become possible.

As usual when trying to solve a problem, more questions than those initially asked arise during the solution process. The case of the control rod cracks is no exception and, as mentioned before, the apparent success of the URANS simulations with the SST $k-\omega$ model raises several questions, namely if this is the merit of the model, and at which Reynolds numbers the URANS approach begins to work, if the associated heat transfer, including temperature fluctuations, is correct, and with which resolutions in time and space, etc. All these questions should be investigated in the future since URANS may constitute a realistic alternative, especially at high Reynolds number, to the promising LES approach that still is too expensive for relatively large applications. Another alternative that has already been used with encouraging results, (Lindqvist, 2011), is Very Large Eddy Simulation (VLES) in the

spirit of Speziale, (Speziale, 1998), an approach which has been further commented by Tinoco et al. (2010c).

Even if LES may be considered in many cases still too resource demanding, it is undeniably the approach of the near future provided that the computer development trend is maintained. However, conjugate heat transfer simulations of industrial applications, i.e. simulations at high Reynolds numbers, involved geometries and complex boundary conditions, appear to lack guidelines for ensuring acceptable quality with a suitable uncertainty. LES, as one of the simulation alternatives for these applications, seems to have taken a first step towards the definition of more complete rules for conjugate heat transfer simulations with the work of Carlsson and Veber (2010). Using a DNS data base for channel flow, (The University of Tokyo, 2012), mesh requirements for LES simulations of heat transfer are established, as functions of the Reynolds and Prandtl numbers. This work should be extended to conjugate heat transfer and temperature fluctuations in the solid by using the results of Tiselj et al. (2001), Tiselj et al. (2004), Tiselj (2011) and Tiselj and Cizelj (2012).

To conclude, this study has tried to show that the analysis of the mechanical integrity of light water reactors as a rather complex task, multidisciplinary and in continuous progress, evolving towards improved safety due to Regulatory demands, new and more advanced methods of analysis and taking advantage of the stably increasing available computer power. Additionally, this work has tried to describe, although incompletely and briefly, the historical progress of the currently accepted methodology and future prospects. Other types of analysis included in the existing methodology, which are not mentioned here due to space limitations, are, for example, studies of thermal loads in transients such as the loss of offsite power (Tinoco et al., 2005) or estimating the moderator tank maximum temperature due to gamma radiation and subcooled boiling heat transfer (Tinoco et al., 2008).

As it might have become apparent from this study, the FEM method for the analysis of structures is considered well established and sufficiently accurate, giving results that do not need verification or experimental validation. The case of three-dimensional numerical computations (CFD) applied to the thermal-hydraulics is very different, mainly due to turbulence, which still lacks an explanatory theory, and to the presence of two-phase flows where the knowledge about the physical processes involved is far from complete. Therefore, the results obtained using three-dimensional numerical computations require validation or at least verification, which is not always possible for complex systems such as nuclear reactors, an issue that has been discussed by Tinoco et al. (2010c).

Author details

Hernan Tinoco^{1,2}

1 Forsmarks Kraftgrupp AB, Sweden

2 Onsala Ingenjörbyrå AB, Sweden

References

- [1] Ahlinder, S., Tinoco, H. and Ullberg, M., (2007). "CFD Analysis of Recombination by HWC in the Downcomer of a BWR", Proceedings of the 12th International Topical Meeting on Nuclear Reactor Thermal Hydraulics (NURETH-12), Pittsburgh, Pennsylvania, U.S.A., September 30-October 4, 2007.
- [2] Angele, K., Odemark, Y., Cehlin, M., Hemström, B., Högström, C.-M., Henriksson, M., Tinoco, H. and Lindqvist, H., (2011). "Flow Mixing Inside a Control-Rod Guide Tube – Part II: Experimental Tests and CFD", Nuclear Eng. Design, Vol. 241, Issue 12, December, 2011.
- [3] ANSI/ANS, (1983a). "Nuclear Safety Criteria for the Design of Stationary Pressurized Water Reactor Plants", ANSI/ANS-51.1-1983.
- [4] ANSI/ANS, (1983b). "Nuclear Safety Criteria for the Design of Stationary Boiling Water Reactor Plants", ANSI/ANS-52.1-1983.
- [5] ANSI/ANS, (1988). "Design Basis for Protection of Light Water Nuclear Power Plants Against the Effects of Postulated Pipe Rupture", ANSI/ANS-58.2-1988.
- [6] ASME, (2010). "Boiler and Pressure Vessel Code with ADDENDA, III: Rules for Construction of Nuclear Power Plant Components", 2010 Edition, New York, USA.
- [7] Brodkey, R. S., (1967). The Phenomena of Fluid Motions, Dover, New York, USA.
- [8] Carlsson, F. and Veber, P., (2010). "Heat transfer validation using LES in turbulent Channel flow", Nordic Symposium Kärnteknik, Nuclear Technology 2010, December 2, Stockholm, Sweden.
- [9] Casey, M. and Wintergerste, T., Editors, (2000). "Best Practice Guidelines", ERCOFTAC Special Interest Group on "Quality and Trust in Industrial CFD", SulzerInnotec, Version 1.0, Switzerland.
- [10] Châtelain, A., Ducros, F. and Métais, O., (2003). "LES of conjugate heat-transfer using thermal wall-functions", Proceedings of the D-LES 5 ERCOFTAC Workshop, Munich, Germany, pp. 307-314.
- [11] Craft, T. J., Iacovides, H. and Uapipatanakul, S., (2010). "Towards the development of RANS models for conjugate heat transfer", J. Turbulence, Vol. 11, No. 26, pp. 1-16.
- [12] de Tilly, A., Penot, F. and Tuhault, J. L. (2006). "Instantaneous heat transfer measurements between an unsteady fluid flow and a wall: application to a non-isothermal 2D-mixing tee", Int. Heat Transfer Conf., Australia, IHTC13. p21.80.
- [13] de Tilly, A. and Sousa, J. M. M., (2008a). "An experimental study of heat transfer in a two-dimensional T-junction operating at a low momentum flux ratio", Int. J. Heat Mass Transfer, Vol. 51, pp. 941-7.

- [14] de Tilly, A. and Sousa, J. M. M., (2008b). "Measurements of instantaneous heat transfer in a two-dimensional T-junction using a multi-thermocouple probe", *Meas. Sci. Technol.*, Vol. 20, pp. 045106-1 – 045106-9.
- [15] Dimotakis, P. E., (2005). "Turbulent Mixing", *Annual Rev. Fluid Mech.* 37:329-56.
- [16] Ellenberger, J. P., Chuse, R., Carson, B., (2004). "Pressure Vessels the ASME Code Simplified", Eighth Edition, McGraw-Hill, New York, USA.
- [17] EU, (1997). "The Pressure Equipment Directive (PED)" (97/23/EC), EU home page, http://ec.europa.eu/enterprise/sectors/pressure-and-gas/documents/ped/index_en.htm.
- [18] European Commission, (2005). "ECORA - Evaluation of Computational Fluid Dynamics Methods for Reactor Safety Analysis", Condensed Final Summary Report, <https://domino.grs.de/ecora/ecora.nsf/>.
- [19] ForsmarksKraftgrupp, (2007). "Forsmark 1 – KFM - Design Specifications for pressure- and force-bearing components of system 415 – Feedwater System", Forsmark Report F1-KFM-415 (in Swedish), 12 June, 2007.
- [20] Forsmarks Kraftgrupp, (2009). "Forsmark 3 – System 30-222, Control Rods. Restart of Forsmark 3 after the refuelling outage of 2009 – Analysis with respect to mechanical integrity", Report FT-2009-2723 (in Swedish), Forsmark, Sweden.
- [21] Hemström, B., Lundström, A., Tinoco, H. and Ullberg, M., (1992). "Flow field dependence of reactor water chemistry in BWR", Proceedings of the 6th International Conference on Water Chemistry of Nuclear Reactor Systems, British Nuclear Energy Society, Bournemouth, 12-15 October, 1992.
- [22] Hermansson, M. and Thorsson, A., (1997). "Forsmark 1 and 2 – Core grid. System 212.3. Dynamic Analysis of Reactor Pressure Vessel with Internals. Response Spectra and forces in core grid for load cases SSE, SRV-1, SRV-12, CO, Chugging and PBI." Forsmark report FT-1997-442, rev 3.
- [23] Hill, R. S., (2008). "Section III – Component Design and Construction", Supporting New Build and Nuclear Manufacturing in South Africa, ASME Nuclear Codes and Standards Workshop, Sandton, South Africa, October 7 – 8, 2008.
- [24] Hosseini, S. M., Yuki, H., and Hashizume, H., (2008). "Classification of Turbulent Jets in a T-Junction Area with a 90-deg Bend Upstream", *Int. J. Heat Mass Transfer*, Vol. 51 (9-10), pp. 2444–2454.
- [25] Hosseini, S. M., Yuki, H., and Hashizume, H., (2009). "Experimental Investigation of Flow Field Structure in Mixing Tee" *J. Fluids Eng.*, Vol. 131, pp. 051103-1 - 051103-7.
- [26] IAEA, (2010), "Safety Classification of Structures, Systems and Components in Nuclear Power Plants", IAEA Safety Standards, DS367.

- [27] Jayaraju, S. T., Komen, E. M. J. and Baglietto, E., (2010). "Suitability of wall-functions in Large Eddy Simulations for thermal fatigue in a T-junction", *Nuc. Eng. Design*, Vol. 240, pp. 2544-2554.
- [28] Johnson, R. W., Schultz, R. R., Roache, P. J., Celik, I. B., Pointer, W. D. and Hassan, Y. A., (2006). "Processes and Procedures for Application of CFD to Nuclear Reactor Safety Analysis", Idaho National Laboratory, Report INL/EXT-06-11789, USA, September 2006.
- [29] Kasagi, N., Kuroda, A., and Hirata, M., (1989). "Numerical Investigation of Near-Wall Turbulent Heat Transfer Taking Into Account the Unsteady Heat Conduction in the Solid Wall," *J. Heat Transfer*, Vol. 111, pp. 385–392.
- [30] Keshmiri, A., (2006). "Modelling of Conjugate Heat Transfer in Near-Wall Turbulence", MSc Thesis, University of Manchester, UK.
- [31] Kuhn, S., Braillard, O., Ničeno, B. and Prasser, H.-M., (2010). "Computational study of conjugate heat transfer in T-junctions", *Nuc. Eng. Design*, Vol. 240, pp. 1548-1557.
- [32] Kukukova, A., Aubin, J. and Kresta, S., (2009). "A new definition of mixing and segregation: Three dimensions of a key process variable", *Chem. Eng. Res. Design*, Vol. 87, No. 4, pp. 633-647.
- [33] Lahey, R. T. and Moody, F. J., (1993). "The Thermal-Hydraulics of a Boiling Water Nuclear Reactor", ANS, La Grange Park, Illinois, USA.
- [34] Lindqvist, H., (2011). "CFD Simulation on Flow Induced Vibrations in High Pressure Control and Emergency Stop Turbine Valve", 14th International Topical Meeting on Nuclear Reactor Thermalhydraulics, NURETH-14, Toronto, Ontario, Canada, September 25-30, 2011.
- [35] Lirvat, J., Mendonça, F., Veber, P. and Andersson, L., (2012). "Flow and Acoustic Excitation mechanisms in a Nuclear Reactor Steam-line and Branch Network", 18th AIAA/CEAS Aeroacoustics Conference, Colorado Springs, Colorado, USA, 4–6 June 2012.
- [36] Menter, F., (2002). "CFD Best Practice Guidelines for CFD Code Validation for Reactor-Safety Applications", UE/FP5 ECORA Project "Evaluation of computational fluid dynamic methods for reactor safety analysis", EVOL-ECORA-D01, Germany.
- [37] Mosyak, A., Pogrebnyak, E., and Hetsroni, G., (2001). "Effect of Constant Heat Flux Boundary Condition on Wall Temperature Fluctuations," *ASME J. Heat Transfer*, Vol. 123, pp. 213–218.
- [38] Muramatsu, T., (2003). "Generation Possibilities of Lower Frequency Components in Fluid Temperature Fluctuations Related to Thermal Striping Phenomena", Transactions of the 17th International Conference on Structural Mechanics in Reactor Technology (SMIRT 17), Prague, Czech Republic, August 17-22, 2003.

- [39] Naik-Nimbalkar, V. S., Patwardhan, A. W., Banerjee, I., Padmakumar, G. and Vaidyanathan, G., (2010). "Thermal Mixing in T-junctions", *Chem. Eng. Science*, Vol. 65, pp. 5901-5911.
- [40] OECD/NEA, (2011). "Report of the OECD-NEA-Vattenfall T-Junction Benchmark exercise", Report NEA/CSNI/R(2011)5, 12 May, 2011.
- [41] Ogawa, H., Igarashi, M., Kimura, N. and Kamide, H., (2005). "Experimental Study on Fluid Mixing Phenomena in T-pipe Junction with Upstream Elbow", Proceedings of the 11th International Topical Meeting on Nuclear Reactor Thermal Hydraulics (NURETH 11), Popes Palace Conference Center, Avignon, France, October 2-6, 2005.
- [42] Pasutto, T., Péniguel, C. and Sakiz, M., (2006). "Chained Computations Using an unsteady 3D Approach for the Determination of Thermal Fatigue in a T-Junction of a PWR Nuclear Plant", *Nuc. Eng. Tech.*, Vol. 38, No. 2, pp. 147-154.
- [43] Polyakov, A. F., (1974). "Wall Effect of Temperature Fluctuations in the Viscous Sub-layer", *Teplofizika Vysokih Temperatur*, Vol. 12, pp. 328-337.
- [44] Pozorski, J. and Minier, J.-P., (2005). "Stochastic Modelling of Conjugate Heat Transfer in Near-Wall Turbulence", *Engineering Turbulence Modelling and Experiments 6*, W. Rodi Editor, Elsevier, pp. 803-812.
- [45] Speziale, C., (1998). "Turbulence Modeling for Time-Dependent RANS and VLES: A Review", *AIAA Journal*, Vol. 36, No.2, pp.173-184.
- [46] STUK, (2000). "Nuclear Power Plant Systems, Structures and Components and their Safety Classification", Guide YVL 2.1, 26 June, 2000.
- [47] Taler, J., Cebula, A., Marcinkiewicz, J. and Tinoco, H., (2011). "Heat Flux and Temperature Determination on the Control Rod Outer Surface", 14th International Topical Meeting on Nuclear Reactor Thermalhydraulics, NURETH-14, Toronto, Ontario, Canada, September 25-30, 2011.
- [48] The Marviken Full Scale Critical Flow Tests, (1979). "Summary Report, Joint Reactor Safety Experiments in the Marviken Power Station", StudsvikEnergiteknik A.B., Nyköping, December 1979, Sweden.
- [49] The University of Tokyo, (2012). Department of Mechanical Engineering, Turbulence and Heat Transfer Laboratory, <http://www.thtlab.t.u-tokyo.ac.jp/>.
- [50] Tinoco, H., (2001). "A Standing Pressure Wave Hypothesis of Oscillating Forces Generated During a Steam-Line Break", proceedings of the 9th International Conference on Nuclear Engineering (ICONE 9), Nice, France, April 8-12, 2001.
- [51] Tinoco, H., (2002). "Three-Dimensional Modeling of a Steam-Line Break in a Boiling Water Reactor", *Nuclear Sci. and Eng.*, Vol. 140, pp. 152-164.
- [52] Tinoco, H., Adolfsson, E., Baltyn, W. and Marcinkiewicz, J., (2005). "BWR ECCS – Thermal Loading Analysis of Internals Related to Spray System Removal", proceed-

- ings of the 13th International Conference on Nuclear Engineering (ICONE 13), Beijing, China, May 16-20, 2005.
- [53] Tinoco, H., Ahlinder, S. and Hedberg, P., (2008). "Estimate of Core Shroud Temperature by means of a CFD-Model of the Core Bypass", proceedings of the 15th International Conference on Nuclear Engineering (ICONE 15), Nagoya, Japan, April 22-26 (2007) and Journal of Power and Energy Systems, Vol. 2, No. 2, pp. 775-789, 2008.
- [54] Tinoco, H. and Lindqvist, H., (2009). "Thermal Mixing Instability of the Flow Inside a Control-Rod Guide Tube", proceedings of the 13th International Topical Meeting on Nuclear Reactor Thermal Hydraulics (NURETH 13), Kanazawa City, Ishikawa Prefecture, Japan, September 27-October 2, 2009.
- [55] Tinoco, H. and Ahlinder, S., (2009). "Mixing Conditions in the Lower Plenum and Core Inlet of a BWR", J. Eng. Gas Turbines & Power, Vol. 131, 062903-1 - 062903-12, November, 2009.
- [56] Tinoco, H., Buchwald, P. and Frid, W., (2010a). "Numerical Simulation of Boron Injection in a BWR", Nuclear Eng. Design, Vol. 240, Issue 2, February, 2010.
- [57] Tinoco, H., Lindqvist, H., Odemark, Y., Högström, C.-M., Hemström, B. and Angele, K., (2010b). "Flow Mixing Inside a Control-Rod Guide Tube – Part I: CFD Simulations", Proceedings of the 18th International Conference on Nuclear Engineering (ICONE 18), Xi'an, China, May 17-21, 2010.
- [58] Tinoco, H., Lindqvist, H. and Frid, W., (2010c). "Numerical Simulation of Industrial Flows", Numerical Simulations - Examples and Applications in Computational Fluid Dynamics, Lutz Angermann (Ed.), ISBN: 978-953-307-153-4, InTech, Available from: <http://www.intechopen.com/books/numerical-simulations-examples-and-applications-in-computational-fluid-dynamics/numerical-simulation-of-industrial-flows>.
- [59] Tiselj, I., Bergant, R., Mavko, B., Bajsić, I. and Hetsroni, G., (2001). "DNS of turbulent heat transfer in channel flow with heat conduction in the wall", J. Heat Transfer – Transactions of ASME, Vol. 123 (5), pp. 849-857.
- [60] Tiselj, I., Horvat, A., Mavko, B., Pogrebnyak, E., Mosyak, A. and Hetsroni, G., (2004). "Wall properties and heat transfer in near wall turbulent flow", Numerical Heat Transfer A, Vol. 46, pp. 717-729.
- [61] Tiselj, I. (2011). "DNS of Turbulent Channel Flow at $Re_T = 395, 590$ and $Pr = 0.01$ ", 14th International Topical Meeting on Nuclear Reactor Thermalhydraulics (NURETH-14), Toronto, Ontario, Canada, September 25-30, 2011.
- [62] Tiselj, I. and Cizelj, L., (2012). "DNS of turbulent channel flow with conjugate heat transfer at Prandtl number 0.01", Nuc. Eng. Design - in print.
- [63] USGenWeb, (2011). "The R. B. Grover & Company Shoe Factory Boiler Explosion", <http://plymouthcolony.net/brockton/boiler.html>.

- [64] vanHaren, S. W. (2011). "Testing DNS capability of OpenFOAM and STAR-CCM+", Master Thesis, University of Delft, September 15, 2011.
- [65] Varrasi, J., (2005). "The True Harnessing of Steam", Mechanical Eng. Mag., January 2005, New York, USA.
- [66] Westin, J., 't Mannetje, C., Alavyoon, F., Veber, P., Andersson, L., Andersson, U., Eriksson, J., Henriksson, M., & Andersson, C., (2008). "High-cycle thermal fatigue in mixing tees. Large-eddy simulations compared to a new validation experiment", proceedings of the 16th International Conference on Nuclear Engineering (ICONE 18), Orlando, Florida, USA, May 11-15, 2008.
- [67] Zeng, L., Jansson, L.G. and Dahlström, L., (2011). "Non-Linear Design Evaluation of Class 1-3 Nuclear Power Piping", Nuclear Power - System Simulations and Operation, PavelTsvetkov (Ed.), ISBN: 978-953-307-506-8, InTech, Available from: <http://www.intechopen.com/books/nuclear-power-system-simulations-and-operation/non-linear-design-evaluation-of-class-1-3-nuclear-power-piping>.

